

Integration of Groundwater Storage and Heat Pumps in Second-Generation District Heating Systems

*Original*

Integration of Groundwater Storage and Heat Pumps in Second-Generation District Heating Systems / Capone, Martina; Verda, Vittorio. - In: JOURNAL OF SUSTAINABILITY FOR ENERGY. - ISSN 2958-1907. - 3:4(2024), pp. 278-286. [10.56578/jse030406]

*Availability:*

This version is available at: 11583/2997727 since: 2025-02-21T17:16:16Z

*Publisher:*

ACADlore

*Published*

DOI:10.56578/jse030406

*Terms of use:*

This article is made available under terms and conditions as specified in the corresponding bibliographic description in the repository

*Publisher copyright*

(Article begins on next page)



# Integration of Groundwater Storage and Heat Pumps in Second-Generation District Heating Systems

Martina Capone<sup>\*</sup>, Vittorio Verda<sup>\*</sup>

Energy Department, Politecnico di Torino, 10129 Torino, Italy

<sup>\*</sup> Correspondence: Martina Capone (martina.capone@polito.it)**Received:** 10-20-2024**Revised:** 11-21-2024**Accepted:** 11-29-2024**Citation:** M. Capone and V. Verda, "Integration of groundwater storage and heat pumps in second-generation district heating systems," *J. Sustain. Energy*, vol. 3, no. 4, pp. 278–286, 2024. <https://doi.org/10.56578/jse030406>.

© 2024 by the authors. Licensee Acadlore Publishing Services Limited, Hong Kong. This article can be downloaded for free, and reused and quoted with a citation of the original published version, under the CC BY 4.0 license.

**Abstract:** District heating (DH) systems in Europe predominantly belong to the second and third generations, operating at temperatures often exceeding 100°C, which poses challenges for integrating renewable energy sources (RES). The feasibility of incorporating large-scale groundwater heat pumps into such systems was explored in this study, with a focus on adjusting the supply water temperature to thermal substations. This adjustment, achieved by lowering the temperature below design values in response to rising outdoor temperatures, facilitated the integration of RES and improved system efficiency. Additionally, groundwater or geothermal heat pumps enabled the effective utilisation of waste heat (WH) from industrial processes or excess heat from renewable sources, particularly during periods when the thermal demand of the DH system was insufficient to justify direct supply. This excess heat, once collected, can be stored in the ground and later retrieved for use during the heating season, contributing to the system's overall sustainability. The integration of seasonal thermal storage further enhances the operational flexibility of DH systems by allowing for the balancing of supply and demand over extended periods. The findings underscore the technical viability and environmental benefits of such integration, providing a pathway for the modernisation of DH infrastructure and the advancement of energy transition goals.

**Keywords:** District heating decarbonisation; Groundwater heat pumps; Supply temperature reduction; Seasonal thermal storage

## 1 Introduction

In its 2023 Energy Efficiency Directive, the European Commission revised the definition of efficient DH and cooling, setting progressive targets to be achieved over the coming years [1]. These targets include at least 50% RES, 50% WH, 75% combined heat and power (CHP) or 50% of a combination of them before 2028; at least 50% RES, 50% WH, 80% high-efficiency combined heat and power (HECHP) or 50% combination of them with at least 5% RES or WH before 2035; at least 50% RES, 50% WH, 80% HECHP or 80% combination of them with at least 35% RES or WH before 2040; at least 75% RES, 75% WH or 95% combination RES, WH and HECHP with at least 5% RES or WH before 2045; a combination of at least 75% RES and WH before 2045; combination of 100% RES and WH before 2050.

A crucial condition to meet these decarbonisation targets is related with a reduction in the supply temperature of water in the existing systems [2–5]. When most of the large DH was built, it was common to consider design values of the supply temperature above 100°C in order to reduce the circulating mass flow rate and thus the pipe diameters, which is the 2nd generation DH. The 3rd generation DH, characterized with supply temperatures of the order to 90°C, was adopted during the 1970s and 1980s and represents nowadays the majority of existing DH systems. Current design targets, especially in the case of small systems, are the low temperature systems operating at 50–70°C and ultra-low temperature systems operating at 35–50°C [6, 7] as well as neutral DH, operating at about 20–35°C.

A major challenge in this field lies in transitioning second- and third-generation DH systems to lower operating temperatures, enabling the integration of heat from geothermal and solar plants, industrial and commercial excess heat [8–10], and power-to-heat solutions such as heat pumps [11–14]. Reasonable target temperatures for this transition are values of about 60–70°C [15]. The main limitations are associated with the requirements of the heating systems currently installed in the connected buildings (often high-temperature radiators), the size of the heat

exchangers installed in the substations and the pipe diameters of the network [16, 17]. In the case of large networks, where the structure can be considered as composed of a transport network, connecting the various plants to the different areas of the town and multiple distribution networks, each connecting the transport network to the different buildings of an area, a possible approach to overcome the limitations consists of reducing the operating temperatures at a distribution network level. The approach adopted in this study consists of keeping the operating temperature at a transport network level as constant during the heating season, while the temperature in the distribution networks is adjusted according to proper requirements through mixing hot water coming from the transport network and warm water produced by a heat pump. In the case examined in this study, the availability of groundwater [18] was exploited to feed a heat pump as well as to store excess heat when the thermal demand of the network is small.

## 2 Temperature Reduction in the Distribution Network

A large DH network which supplies heating to more than 6,500 buildings was considered. The thermal demand in winter was about 1 GW, with morning peaks reaching 1.4 GW, which was covered using mainly HECHP plants, while thermal storage units covered the peak demand. The supply temperature was kept at about 120°C during the heating season. The distribution network analyzed in this application was very small, consisting of only three office buildings, but it served as the site for the experimental application of the proposed concept. The annual thermal energy request was 945 MWh, while maximum thermal demand (at daily steady state without considering the morning peaks) registered in recent years was about 900 kW and corresponded to an average external temperature of -1.1°C. It should be noted that the external temperature is registered by the temperature sensor used to control the substation and measurements are slightly higher than the real temperature because of the interactions with the building where it is installed.

A steady-state model of the substations, whose characteristics were obtained from measurements, was used to calculate the minimum supply temperature to each building as a function of the external temperature. The available measurements in each operating condition are the water mass flow rate on the DH side ( $G$ ), the four temperatures at the heat exchanger, namely  $T_1$ ,  $T_2$ ,  $T_3$  and  $T_4$  in Figure 1, and the external temperature ( $T_{out}$ ).

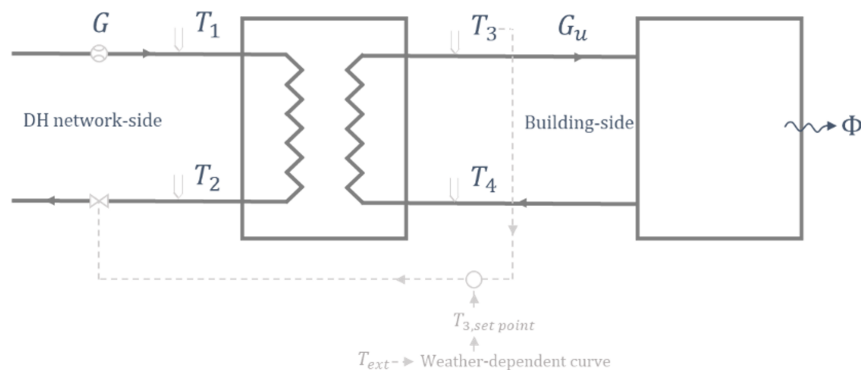


**Figure 1.** Schematic of a thermal substation

The first step of the procedure consists of the evaluation of the energy signature of the buildings, which represents the steady-state thermal demand as the function of the external temperature [19]. The heat flux was evaluated as the product of the mass flow rate on the network times the specific heat of water times the temperature difference on the supply and the return ( $T_1 - T_2$ ). The thermal signature of one of the three buildings connected to the distribution network is shown in subgraph (a) of Figure 2. The available data from the substation was introduced in a mean logarithmic temperature difference expression to obtain the quantity  $UA$ , which is the product of the heat transfer area times the global heat transfer coefficient of the heat exchanger. This is represented in subgraph (b) of Figure 2, which shows that the global heat transfer coefficient increases with the mass flow rate. The mean logarithmic temperature difference model was then used to obtain the mass flow rate required to supply a certain heat flux to the substation depending on the DH supply temperature. This is shown in subgraph (c) of Figure 2, where the model results are compared with the experimental data. This graph shows that, to a certain extent, the network supply temperature which is required to exchange a certain heat flux in the substation can be reduced by increasing the mass flow rate. As the maximum value of the water mass flow rate that can be supplied to a thermal substation is limited by the pipe diameters and the operating condition of the network, the last graph can be used to determine the minimum supply temperature that is required to exchange a certain heat flux. This minimum temperature reduces when the heat demand of the substation reduces, if the circulating mass flow rate is kept to the maximum allowed value.

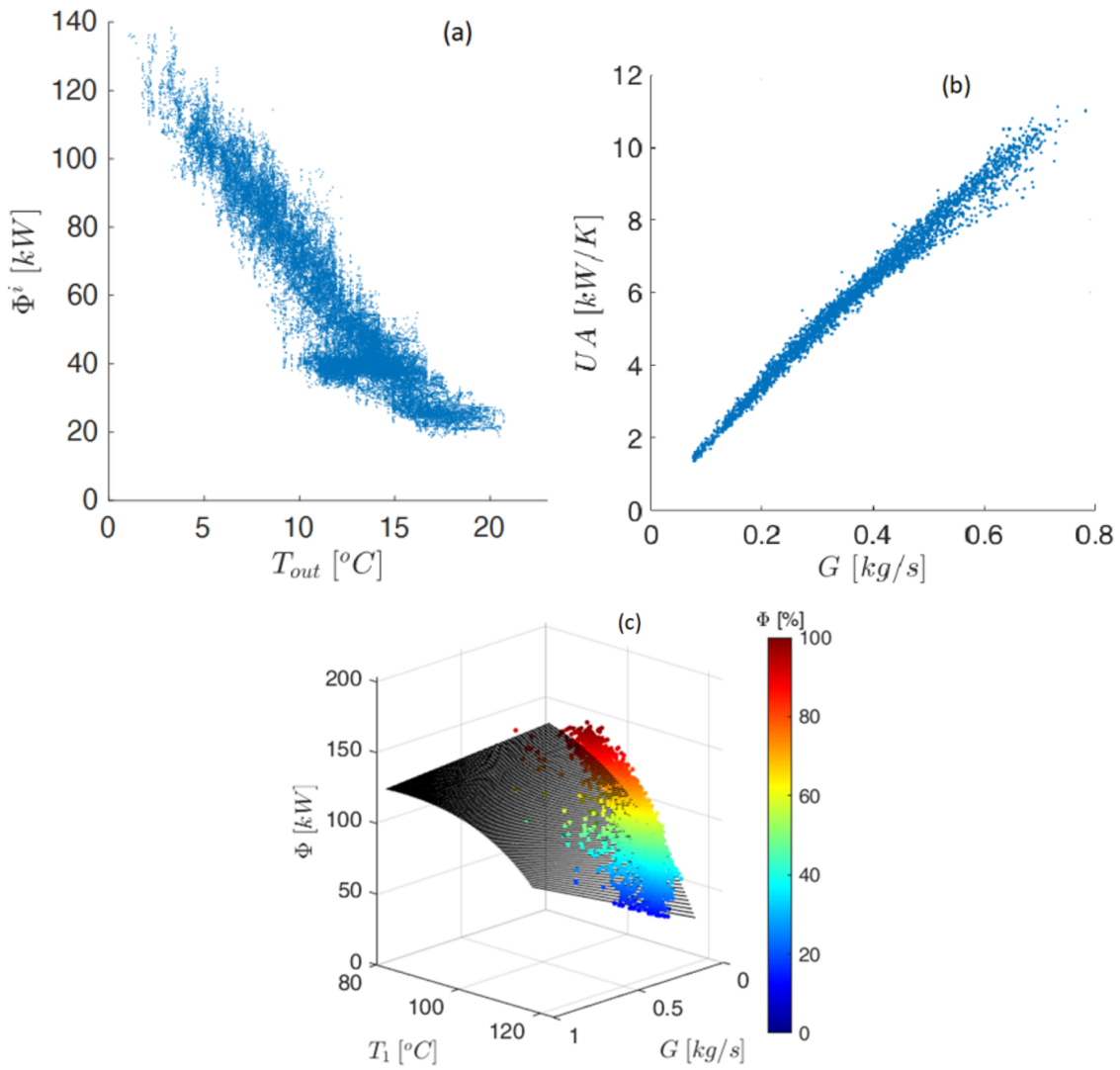


**Figure 2.** Substation model: (a) Thermal demand; (b) Effect of mass flow rate on the global heat transfer coefficient; (c) Operation of the heat exchanger

The analysis was conducted by considering the daily average temperatures along the heating season, as shown in Figure 3.

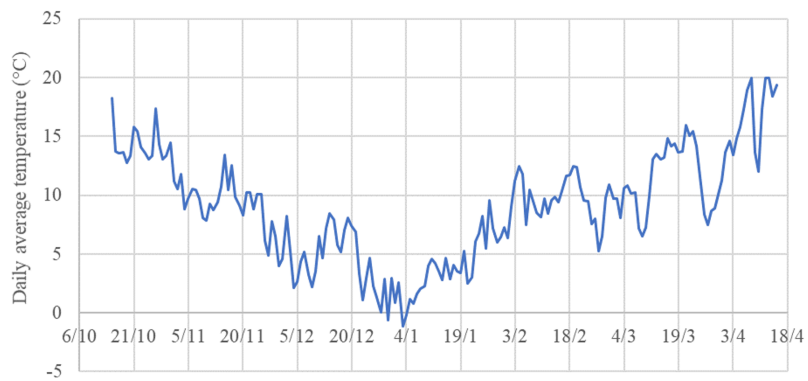


**Figure 3.** Evolution of the average daily temperature along the heating season

### 3 Heat Pump Installation

A groundwater heat pump able to produce up to 350 kW hot water at a maximum temperature of 85°C was installed in the distribution network, as shown in Figure 4. The impact of the size of the heat pump on the decarbonisation was then analyzed. The nominal coefficient of performance (COP) of the heat pump is 2.99 when the supply temperature is 85°C, the return temperature is 70°C and the groundwater temperature is 15°C (undisturbed temperature).

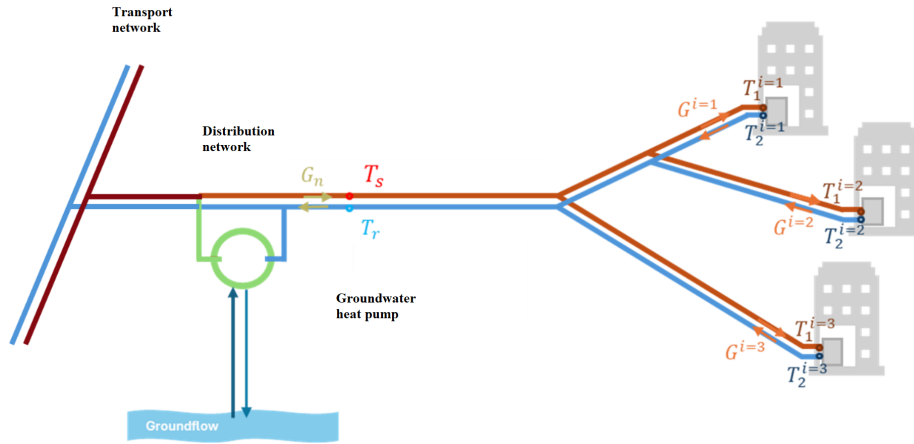


**Figure 4.** Installation of the groundwater heat pump on the distribution network

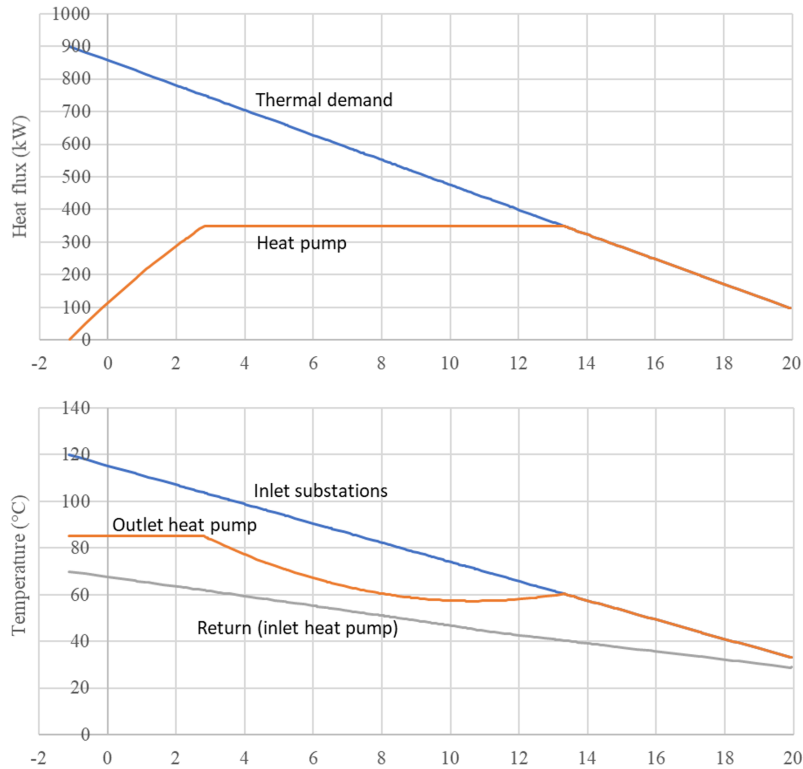


**Figure 5.** Thermal demand of the substations (heat flux and supply temperature) and heat pump operation

The connection to the transport network guarantees that the thermal demand is covered even when the demand is larger than 350 kW and the minimum supply temperature exceeds 85°C. Assuming that  $T_{1,1}$ ,  $T_{1,2}$  and  $T_{1,3}$  are the minimum supply temperatures of the three substations, the supply temperature of the distribution network  $T_s$  was selected as the maximum between these three values. The total heat flux and  $T_s$  were guaranteed by selecting the water mass flow rate extracted from the transport network and the temperature of water exiting the heat pump. Figure 5 shows the heat flux requested by the distribution network as the function of the external temperature and the portion of heat covered by the heat pump (the remaining part is covered by the water extracted from the transport

network). When the external temperature is lower than about 2.5°C, the contribution of the heat pump is lower than 350 kW because the supply temperature to be supplied to the substations exceeds 85°C, as shown in the diagram below. When the external temperature is above 13°C, the heat pump is able to comply the requirements of the substations both in terms of heat flux and supply temperature.

Considering the distribution of the external temperatures along the heating season, the heat pump would operate covering about 62.5% of the heating demand, with an average COP of 3.19, which is larger than the nominal COP due to the fact that the supply temperature reduces when the external temperature is above 2.5°C and the return temperature decreases when the outdoor temperature increases.

The percentage of heat produced from renewable sources is thus between 43% (in the case the electricity feeding the heat pump is not produced from renewable energy) and 62.5%.

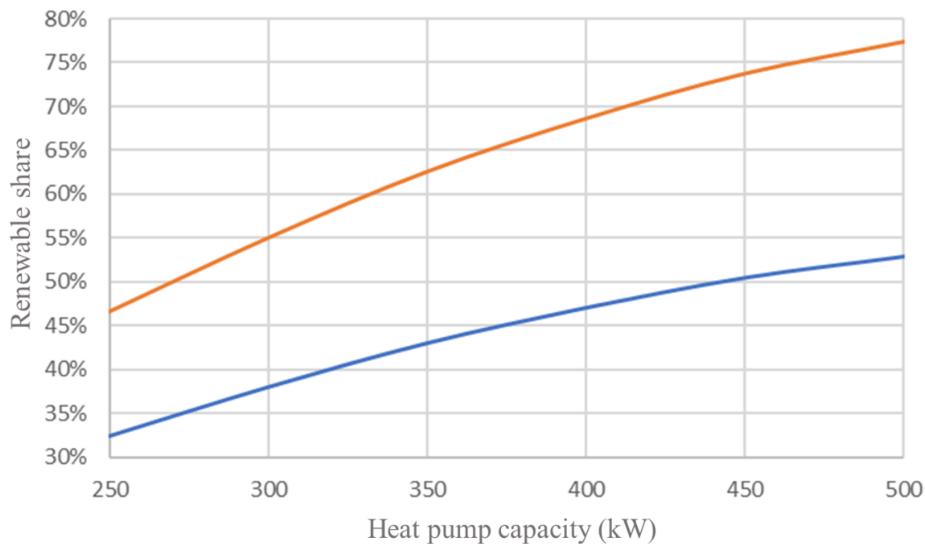


**Figure 6.** Min and max share of renewable energy in the distribution network as the function of the heat pump capacity

Figure 6 analyses the contribution of RES to the total demand in the case of renewable and non-renewable electricity to feed the heat pump, depending on the size of the heat pump. The curve associated with the maximum share is strictly related with the percentage of heat covered by the heat pump; the marginal additional contribution tends to decrease as the heat pump size increases. The curve associated with the minimum share is also affected by the COP of the heat pump. The larger the size, the smaller the average COP, which passes from 3.28 in the case of a 250 kW heat pump to 3.15 in the case of a 500 kW heat pump.

#### 4 Groundwater Flow Modelling

A further improvement that can be implemented in this system consists of the possibility to take advantage of summer operation of the heat pump as a chiller. In this case, the heat released from the condenser can be stored in the groundwater and extracted during the heating season in order to increase the performance of the heat pump. Similar advantage can be obtained by storing in the groundwater excess heat from productive processes, supermarkets or data centres from renewable plants (mainly solar collectors) or heat released from other chillers. As the groundwater in the area considered for the installation is flowing with a velocity of the order of 1-2 m/day, the groundwater extraction must be performed downstream the injection at a proper distance which depends on the time delay between the excess heat availability and its use.

To properly calculate the efficiency of this thermal storage, a computational fluid dynamic model of the subsurface was used. This model considers the momentum and energy equation. Momentum equation is written in the form of the Darcy equation:

$$v = -\frac{k}{\mu} \nabla p \quad (1)$$

where,  $v$  is the velocity vector,  $k$  is the ground permeability,  $\mu$  is dynamic viscosity, and  $p$  is the pressure. Eq. (1) was substituted in the continuity equation, as shown in Eq. (2), to obtain the partial differential equation to be solved, as shown in Eq. (3):

$$\nabla \cdot v = 0 \quad (2)$$

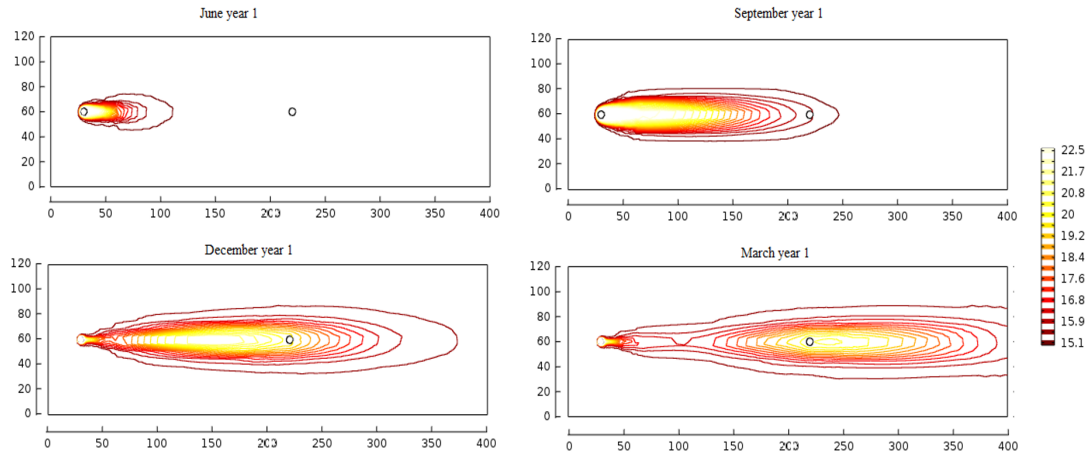


**Figure 7.** Groundwater temperature distribution during the first year operation

$$\frac{k}{\mu} \nabla^2 p = 0 \quad (3)$$

The energy equation is written in transient form:

$$\lambda \nabla^2 T = \rho c v \cdot \nabla T + \rho c \frac{\partial T}{\partial t} \quad (4)$$

where,  $\lambda$  is the equivalent conductivity (considering the contributions of both the soil and water),  $T$  is the temperature,  $\rho$  is the density, and  $c$  is the specific heat. The computational domain which was adopted for the specific installation examined in the present work includes the injection well, the extraction well (located at about 220 m downstream the injection), the unsaturated unit (i.e., the upper portion of the ground without water flow), and the first saturated unit. This model was validated through comparison of the numerical results with the temperature measurements available from piezometers [20].

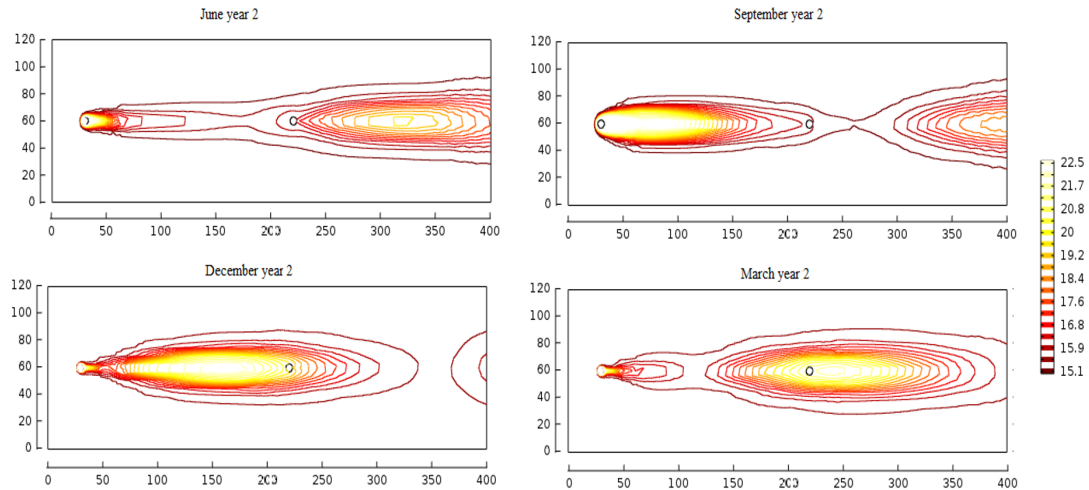


**Figure 8.** Groundwater temperature distribution during the second year operation

The cooling demand for the three buildings was estimated as 325 MWh and occurred in the period between middle May to middle September. The heat injection in the groundwater was estimated as 450 MWh. Figure 7 and Figure 8 show the groundwater thermal plume evolution during the operation of the first and second years in the case the heat injection is combined with an extraction performed according to the heat pump operation presented in Figure 5. The figure also shows the two wells, which are located at a distance of 190 m. When the system operates in cooling mode, the upstream well injects hot water in the groundwater system (which is extracted from a well located upstream and not represented), while during the heating season, the water is extracted from the well located downstream, thus taking advantage of a higher temperature.

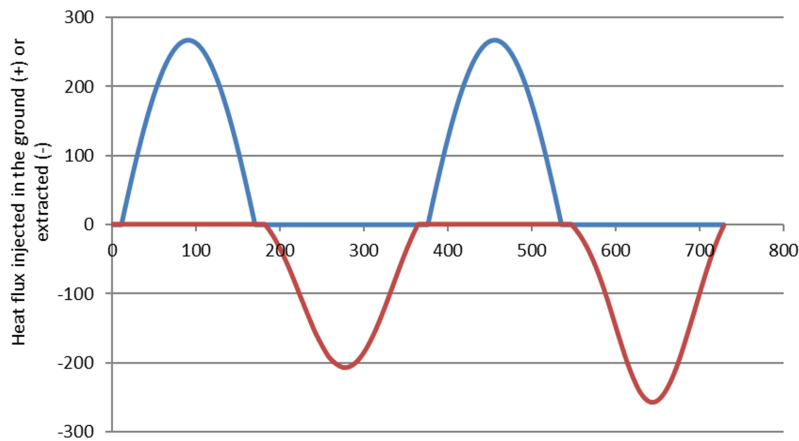


**Figure 9.** Heat flux exchanged with the groundwater

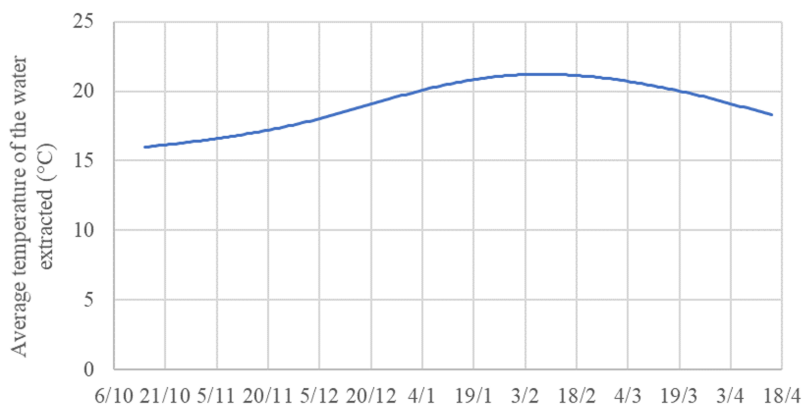


**Figure 10.** Temperature of the extracted groundwater

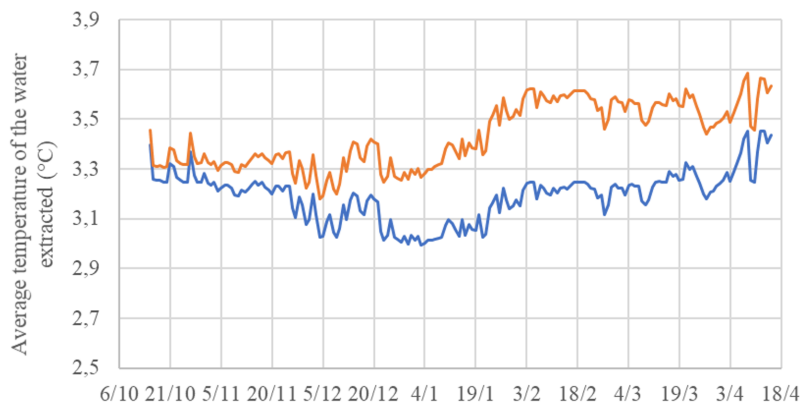


**Figure 11.** Heat flux exchanged with the groundwater

The annual efficiency of the storage system with the examined configuration, calculated as the ratio between the thermal energy associated with the temperature deviation of the water extracted from the ground with respect to the undisturbed temperature (15°C) and the energy injected in the groundwater, is about 85% when evaluated considering two-year operation. Figure 9 shows the heat flux injected in the ground (+) and the heat flux extracted during two-year operation.

The resulting temperature profile of the water extracted from the downstream well during the second heating season is shown in Figure 10, which shows that temperature is always larger than the perturbed value and reaches a maximum of about 21.2°C.

The COP of the heat pump along the first heating season operation is shown in Figure 11, where it is compared with that obtained feeding the heat pump with water at the undisturbed temperature. The average COP increases

from about 3.2 to 3.45, therefore, the minimum contribution to the share of renewable increases from about 0.43 to almost 0.45%.

## 5 Conclusions

In this study, the integration of a groundwater heat pump in the distribution network of a second-generation DH was proposed. The thermal demand of the buildings connected with the DH was managed through proper selection of the supply temperature in the distribution network; requirements in terms of supply temperature and heat demand were fulfilled by mixing water produced at 85°C by the heat pump and water at 120°C available from the transmission network. This approach significantly increased the percentage of heat produced from renewable energy without requiring modifications to the operational settings of building heating systems or substations. Depending on the size of the heat pump, the share of renewable heat supplied to the end-users of the distribution network varied between 33%-47% (in the case of non-renewable electricity and renewable electricity, respectively) to about 53%-77%.

An additional option, which consists of taking advantage of extra heat stored in the groundwater, was also examined. This allows one to further increase the share of renewable energy used to feed the examined portion of DH network. In addition, a further 7% reduction in the electricity consumption of the heat pump was achieved.

## Author Contributions

Conceptualization, M. Capone and V. Verda; methodology, V. Verda; software, M. Capone.; validation, M. Capone; formal analysis, M. Capone; investigation, M. Capone and V. Verda; resources, V. Verda; data curation, V. Verda; writing—original draft preparation, M. Capone; writing—review and editing, M. Capone; visualization, V. Verda; supervision, V. Verda; project administration, V. Verda; funding acquisition, V. Verda. All authors have read and agreed to the published version of the manuscript.” The relevant terms are explained at the CRediT taxonomy.

## Funding

This research is part of a project funded under the National Recovery and Resilience Plan (NRRP), Mission 4 Component 2 Investment 1.3 - Call for tender No. 341 of 15.03.2022 of Ministero dell'Università e della Ricerca (MUR); funded by the European Union – NextGenerationEU. Award Number: Project code PE0000021, Concession Decree No. 1561 of 11.10.2022 adopted by Ministero dell'Università e della Ricerca (MUR), CUP E13C22001890001, Project title “Network 4 Energy Sustainable Transition – NEST”.

## Data Availability

The data used to support the findings of this study are available from the corresponding author upon request.

## Conflicts of Interest

The authors declare no conflicts of interest.

## References

- [1] European Union, “Directive (EU) 2023/1791 of the European Parliament and of the Council of 13 September 2023 on energy efficiency and amending Regulation (EU) 2023/955 (recast) (Text with EEA relevance),” 2023. <https://eur-lex.europa.eu/eli/dir/2023/1791/oj/eng>
- [2] T. Benakopoulos, R. Salenbien, D. Vanhoudt, and S. Svendsen, “Improved control of radiator heating systems with thermostatic radiator valves without pre-setting function,” *Energies*, vol. 12, no. 17, p. 3215, 2019. <https://doi.org/10.3390/en12173215>
- [3] F. Wendel, M. Blesl, L. Brodecki, and K. Hufendiek, “Expansion or decommission?—Transformation of existing district heating networks by reducing temperature levels in a cost-optimum network design,” *Appl. Energy*, vol. 310, p. 118494, 2022. <https://doi.org/10.1016/j.apenergy.2021.118494>
- [4] D. S. Østergaard and S. Svendsen, “Costs and benefits of preparing existing danish buildings for low-temperature district heating,” *Energy*, vol. 176, pp. 718–727, 2019. <https://doi.org/10.1016/j.energy.2019.03.186>
- [5] J. Stock, F. Arjuna, A. Xhonneux, and D. Müller, “Modelling of waste heat integration into an existing district heating network operating at different supply temperatures,” *Smart Energy*, vol. 10, p. 100104, 2023. <https://doi.org/10.1016/j.segy.2023.100104>
- [6] W. Meesenburg, T. Ommen, J. E. Thorsen, and B. Elmegaard, “Economic feasibility of ultra-low temperature district heating systems in newly built areas supplied by renewable energy,” *Energy*, vol. 191, p. 116496, 2020. <https://doi.org/10.1016/j.energy.2019.116496>
- [7] O. Dolna and J. Mikielwicz, “The ground impact on the ultra-low-and low-temperature district heating operation,” *Renew. Energy*, vol. 146, pp. 1232–1241, 2020. <https://doi.org/10.1016/j.renene.2019.07.048>

- [8] D. Moreno, S. Nielsen, P. Sorknæs, H. Lund, J. Z. Thellufsen, and B. V. Mathiesen, “Exploring the location and use of baseload district heating supply. What can current heat sources tell us about future opportunities?” *Energy*, vol. 288, p. 129642, 2024. <https://doi.org/10.1016/j.energy.2023.129642>
- [9] A. M. Jodeiri, M. J. Goldsworthy, S. Buffa, and M. Cozzini, “Role of sustainable heat sources in transition towards fourth generation district heating – A review,” *Renew. Sustain. Energy Rev.*, vol. 158, p. 112156, 2022. <https://doi.org/10.1016/j.rser.2022.112156>
- [10] P. Sorknæs, P. A. Østergaard, J. Z. Thellufsen, H. Lund, S. Nielsen, S. Djørup, and K. Sperling, “The benefits of 4th generation district heating in a 100% renewable energy system,” *Energy*, vol. 213, p. 119030, 2020. <https://doi.org/10.1016/j.energy.2020.119030>
- [11] P. A. Østergaard and A. N. Andersen, “Booster heat pumps and central heat pumps in district heating,” *Appl. Energy*, vol. 184, pp. 1374–1388, 2016. <https://doi.org/10.1016/j.apenergy.2016.02.144>
- [12] M. Capone, E. Guelpa, and V. Verda, “Optimal installation of heat pumps in large district heating networks,” *Energies*, vol. 16, no. 3, p. 1448, 2023. <https://doi.org/10.3390/en16031448>
- [13] B. Bach, J. Werling, T. Ommen, M. Münster, J. M. Morales, and B. Elmegaard, “Integration of large-scale heat pumps in the district heating systems of Greater Copenhagen,” *Energy*, vol. 107, pp. 321–334, 2016. <https://doi.org/10.1016/j.energy.2016.04.029>
- [14] H. Pieper, T. Ommen, B. Elmegaard, and W. B. Markussen, “Assessment of a combination of three heat sources for heat pumps to supply district heating,” *Energy*, vol. 176, pp. 156–170, 2019. <https://doi.org/10.1016/j.energy.2019.03.165>
- [15] H. Lund, P. A. Østergaard, T. B. Nielsen, S. Werner, J. E. Thorsen, O. Gudmundsson, A. Arabkoohsar, and B. V. Mathiesen, “Perspectives on fourth and fifth generation district heating,” *Energy*, vol. 227, p. 120520, 2021. <https://doi.org/10.1016/j.energy.2021.120520>
- [16] E. Guelpa, M. Capone, A. Sciacovelli, N. Vasset, R. Baviere, and V. Verda, “Reduction of supply temperature in existing district heating: A review of strategies and implementations,” *Energy*, vol. 262, p. 125363, 2023. <https://doi.org/10.1016/j.energy.2022.125363>
- [17] M. Capone, E. Guelpa, and V. Verda, “Exploring opportunities for temperature reduction in existing district heating infrastructures,” *Energy*, vol. 302, p. 131871, 2024. <https://doi.org/10.1016/j.energy.2024.131871>
- [18] C. S. Blázquez, V. Verda, I. M. Nieto, A. F. Martín, and D. González-Aguilera, “Analysis and optimization of the design parameters of a district groundwater heat pump system in Turin, Italy,” *Renew. Energy*, vol. 149, pp. 374–383, 2020. <https://doi.org/10.1016/j.renene.2019.12.074>
- [19] M. Capone, E. Guelpa, and V. Verda, “Potential for supply temperature reduction of existing district heating substations,” *Energy*, vol. 285, p. 128597, 2023. <https://doi.org/10.1016/j.energy.2023.128597>
- [20] V. Verda, G. Baccino, A. Sciacovelli, and S. Lo Russo, “Impact of district heating and groundwater heat pump systems on the primary energy needs in urban areas,” *Appl. Therm. Eng.*, vol. 40, pp. 18–26, 2012. <https://doi.org/10.1016/j.applthermaleng.2012.01.047>